

## Deformation-Induced Chemical Inhomogeneity and Short-Circuit Diffusion in Shear Bands of a Bulk Metallic Glass

M. R. Chellali,<sup>1,\*</sup> S. H. Nandam<sup>1</sup> and H. Hahn<sup>1,2</sup>

<sup>1</sup>*Institute of Nanotechnology, Karlsruhe Institute of Technology, 76344 Eggenstein-Leopoldshafen, Germany*

<sup>2</sup>*KIT-TUD Joint Research Laboratory Nanomaterials, Institute of Materials Science, Technical University Darmstadt, 64287 Darmstadt, Germany*



(Received 12 May 2020; accepted 25 September 2020; published 10 November 2020)

The compositional changes in shear bands of a Cu<sub>50</sub>Zr<sub>50</sub> metallic glass after plastic deformation at room temperature have been monitored by atom probe tomography. Across the width of the shear bands an asymmetry of the enriched and depleted zones of the constituent elements is observed, while no change of the composition within the surrounding matrix occurs. The diffusion coefficients determined from the concentration profiles are orders of magnitude larger than the values of bulk diffusion at room temperature. The asymmetric concentration profiles of the constituent elements (Cu and Zr) remain stable during annealing at a temperature of 543 K, even though fast and preferential diffusion of a Ni tracer has been found along the shear band at the same temperature. The results indicate that the atomic structure and stress distribution within the shear bands is altered from that of the surrounding amorphous matrix. The fact that the shear band structure is unaltered at elevated temperatures and that fast diffusion occurs preferentially within the shear bands leads to the conclusion that they are structurally stable.

DOI: [10.1103/PhysRevLett.125.205501](https://doi.org/10.1103/PhysRevLett.125.205501)

Characterizing shear bands at the nanoscale by conventional microscopic tools has proven to be a challenging exercise. For example, even sophisticated electron microscopy techniques do not yield clear images of shear bands and detailed information on the stress fields and composition, even though the existence of surface steps clearly indicates the presence of shear bands [1,2]. Consequently, theoretical modeling and atomistic simulation have been the methods of choice to obtain structural details of the shear band structure [2,3]. A few experimental studies on the local structure of shear bands have been reported in the literature; these studies have used electron acoustic emission spectroscopy [4,5] and high-resolution transmission electron microscopy (TEM) [1,6] for the structural analysis of the bands. To better elucidate the structural features and especially to examine the possible presence of free volume, understanding of the interrelation between the bulk and shear bands transport in plastically deformed metallic glasses becomes of particular interest [7,8]. Recently, Bokeloh *et al.* [9] found that in Pd<sub>40</sub>Ni<sub>40</sub>P<sub>20</sub> metallic glass, the Ag-diffusion coefficients were several orders of magnitude higher in the shear bands than in the bulk. The enhanced atomic diffusivity was hypothesized to result from either the presence of local free volume inside the bands or at the interfaces between the shear bands and the undeformed matrix. In a subsequent study by the same group, correlative high-angle annular dark-field scanning transmission electron microscopy was employed to reveal alternating changes of free volume along specified shear bands and thus clearing the ambiguity from their earlier

hypothesis [1]. Surprisingly, to date, no self-diffusion and interdiffusion experiments have been reported in the shear band of a deformed bulk metallic glass. To the best of our knowledge, the present report is the first comprehensive study on the deformation-induced changes that give rise to very fast self- and impurity diffusion rates along shear bands in bulk metallic glasses at liquid nitrogen, room and high temperatures.

A binary (Cu-Zr) glass-forming system was prepared by a standard melt-spinning technique in the argon atmosphere [10]. In Supplemental Material (SM) [11], the amorphous nature of the as-prepared Cu<sub>50</sub>Zr<sub>50</sub> melt-spun ribbon is confirmed by x-ray diffraction, which shows the broad peak typical for metallic glasses (Fig. SM1a). After applying Vickers indentation (500 gf) on the ribbon, shear bands are obvious around the pileup region (Fig. SM1b). Figure SM1c shows a lamella extracted from the vicinity of the indentation mark parallel to the shear bands, which is welded to an Omniprobe needle and attached to a LEAP microtip post. The shear bands are clearly identified exiting at the surface next to the indenter and also below the indenter. Atom probe tomography (APT) samples were prepared exclusively from the region below the indent (see arrows in Figs. SM1b and SM1c) [11]. Figure SM1d shows an individual mount cut free from the wedge containing a shear band indicated by arrows. Figure SM1e shows a SEM image of APT tip with a diameter smaller than 60 nm, which is sufficient for subsequent field evaporation [12,13].

A 3D atomic reconstruction of a tip with a shear band in the deformed Cu<sub>50</sub>Zr<sub>50</sub> metallic glass is seen in Fig. 1(a)

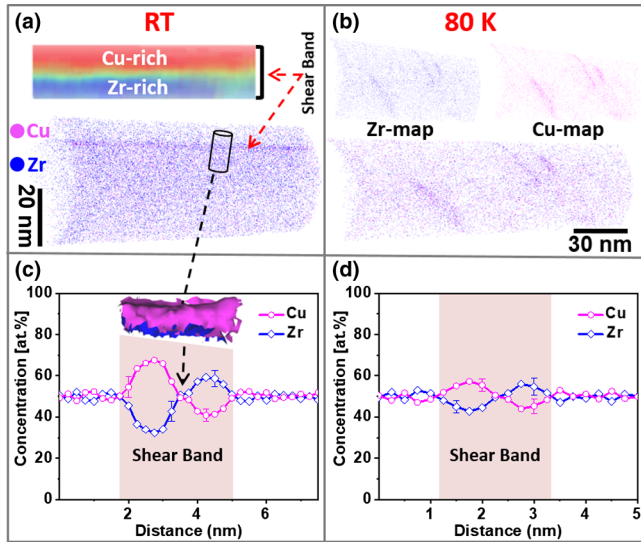


FIG. 1. (a) APT reconstruction of the deformed  $\text{Cu}_{50}\text{Zr}_{50}$  ribbon containing a shear band (bottom). 2D composition heat map taken along the plane perpendicular to the viewing direction inside the band (top). Color code: (36 at. % = blue, 69 at. % = red) for Cu (bottom). Clearly, Cu- and Zr-rich compositions are observed in the band as indicated by the red arrows in Fig. 1(a). The 2D composition heat map represents the distribution of the Cu concentration in the shear band as represented in the top part of Fig. 1(a). (b) APT reconstruction of an indentation made at nominal temperature of 80 K containing shear bands. 1D concentration profiles are shown within the shear band at (c) RT and (d) 80 K. Error bars mark the  $1\sigma$  range. The cylinder (diameter, 6 nm) drawn in (a) shows the section used in the analysis. The inset of (c) shows the chemical isosurfaces associated with Cu (56 at. %) and Zr (56 at. %) highlighting the shear band.

(bottom). Clearly, Cu- and Zr-rich compositions are observed in the band as indicated by the red arrows in Fig. 1(a). The 2D composition heat map represents the distribution of the Cu concentration in the shear band as represented in the top part of Fig. 1(a).

In order to address whether these structural changes may be due to heating during the shear band formation, the as-prepared  $\text{Cu}_{50}\text{Zr}_{50}$  metallic glass ribbon was inserted into liquid nitrogen for 10 min. Immediately ( $\leq 20$  s) after removing from the liquid nitrogen, the sample was deformed by indentation. Subtle segregation of Cu and Zr within the shear band is observed [Fig. 1(b)], which can be clearly resolved from the elemental maps of Cu (upper right) and Zr (upper left). In Fig. SM2a, an atomic reconstruction of undeformed region, which was taken near the indent without any shear bands at room temperature (RT) is shown as a reference [11]. No indication of any significant chemical fluctuations was observed as illustrated in Fig. SM2b [11]. By cutting local cylinders of analysis perpendicular to the shear band, as shown in the Fig. 1(a), the composition profile across the shear band is determined [Fig. 1(c)]. While the undeformed sample shows only negligible compositional fluctuations (Fig. SM2b), the concentration profiles across the shear bands give clear evidence for marked enrichments of Cu ( $\sim 69$  and 57 at. % at RT and 80 K, respectively) and Zr

( $\sim 63$  and  $\sim 56$  at. % at RT and 80 K, respectively). In the inset of Fig. 1(c), the isoconcentration surfaces of Cu and Zr are constructed at 56 at. %. The compositional profiles are highly asymmetric, i.e., one side of the shear band is enriched with Cu (depleted in Zr), while the other side is rich in Zr (depleted in Cu). The total width of the enrichment-depletion zones is found to be  $\sim 4$  nm. The concentration profiles across the shear bands for the deformed sample at 80 K [Fig. 1(d)] show lower redistribution than those deformed at RT [Fig. 1(c)]. However, the present experiments could not allow us to directly determine whether Cu or Zr enrichment or depletion occurred toward the indent side or away from it.

In order to test the thermal stability of the compositional changes in the shear bands, the samples were annealed at two different temperatures, 120 and 15 min at 523 and 543 K, respectively. Prior to the annealing, the deformed sample was coated with a thin layer of Ni, which allows us to trace its diffusion path. The APT measurements were analyzed in two different regions, see Fig. 2(a): (1) deep into the shear band (without any Ni) and (2) at the regions of the shear band close to the surface. From (1), the stability of the compositional changes in the shear band can be determined, while (2) allows the comparison of the Ni diffusivity in the shear band and its adjacent regions. From Fig. 2(a) it is evident that the Ni diffusion is restricted to the narrow range inside the shear band.

To investigate the stability of the shear band at 523 and 543 K, the concentration depth profiles are measured through a cylindrical volume across the shear band [see misty rose cylinder in Fig. 2(a)] as shown in Figs. 2(b) and SM3a [11]. At both temperatures, the concentration

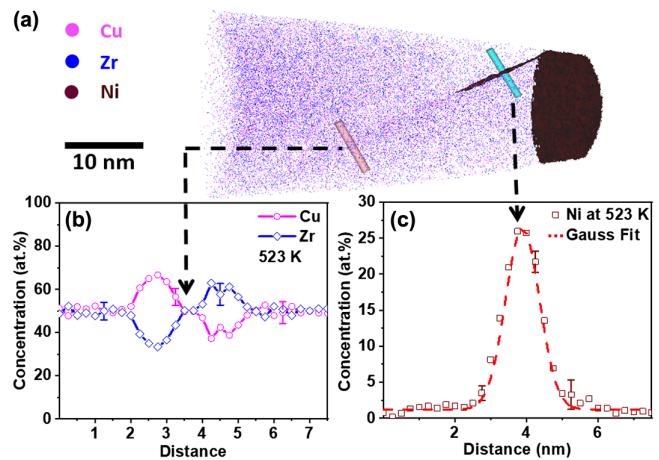


FIG. 2. (a) Atomic reconstruction of a Cu-Zr metallic glass with a top Ni layer after annealing at 523 K for 120 min, overlaid with the isoconcentration surface of Ni (17 at. %), showing the preferential diffusion of Ni along shear band. Composition profile across the shear band in (b) the region without Ni and (c) the Ni-enriched zone with a fit using a Gaussian distribution. Error bars mark the  $1\sigma$  range. Positions of the analysis cylinders (diameter, 6 nm) are sketched in (a).

redistributions in the shear band remain almost identical to the composition fluctuations at RT [see Fig. 1(c)]. This observation clearly indicates that shear bands are structurally stable, i.e., do not relax back to the original amorphous structure and homogeneous composition, even at temperatures as high as 543 K. In order to calculate the Cu/Zr self-diffusion coefficients, the time of diffusion is required. However, it is not clear which time to choose: anything between the duration of shear band motion to the time difference between the deformation and the measurement of the concentration profile could be acceptable. Additionally, the concentration profiles of Cu and Zr within the shear band are stable at RT and even at 543 K, indicating slow diffusion at this temperature and time range, leading to the conclusion that the redistribution of Cu and Zr atoms actually occurs on a rather short timescale during the shear band motion. The relatively large concentration changes over a narrow range around the center of the shear band can of course be caused by alternative mechanisms other than diffusion or are an indication of extremely high temperatures reached within the shear band during its motion [14]. Therefore, for the estimate of a lower limit of effective diffusion coefficients a long time of 10 s is assumed. As a consequence, the value of the diffusion coefficient of both elements in the metallic glass is calculated using the measured parameters for each element. The Cu diffusion coefficient is determined to be  $D_{\text{Cu}}^{\text{SB}} 4.82 \times 10^{-15} \text{ cm}^2/\text{s}$ , which is 11 orders of magnitude faster than the Cu self-diffusion at RT in crystalline copper [15]. In the same manner, Cu and Zr self-diffusion coefficients are measured for both temperatures (RT, 80 K) across the shear bands [Fig. 3(b)]. It is observed that Cu ( $D_{\text{Cu-RT}}^{\text{SB}} = 4.82 \times 10^{-15} \text{ cm}^2/\text{s}$ ,  $D_{\text{Cu-80K}}^{\text{SB}} = 3.6 \times 10^{-16} \text{ cm}^2/\text{s}$ ) has higher diffusivity than Zr ( $D_{\text{Zr-RT}}^{\text{SB}} = 1.6 \times 10^{-16} \text{ cm}^2/\text{s}$ ,  $D_{\text{Zr-80K}}^{\text{SB}} = 2.25 \times 10^{-17} \text{ cm}^2/\text{s}$ ). Similar differences have been attributed to the size dependence of the diffusing elements in Ni-Zr metallic glasses [16]. In analogy to amorphous Ni-Zr, it is expected that the smaller Cu atoms diffuse faster than the larger Zr atoms, as observed in the present experiments.

Now to study the Ni diffusion along the shear band, an atomic-scale imaging, showing the isoconcentration contours of the Ni after annealing for 120 min at 523 K is plotted in Fig. 2(a). At an isoconcentration surface of 17 at. % Ni, the Ni-enriched zones are clearly visible along the shear band. By placing a perpendicular cylinder to the shear band in the Ni-diffused zone [see the blue cylinder in Fig. 3(a)], the Ni-concentration profile across the shear band can be resolved. Two examples obtained after 120 and 15 min annealing at 523 and 543 K, respectively, are shown in Fig. 2(c) and Fig. SM3b [11]. The profiles, which can be reasonably fitted using a Gaussian solution, have considerable width of about 2 and 2.4 nm at 523 [Fig. 2(c)] and 543 K (Fig. SM3b) [11], respectively. Interestingly, the Ni atoms diffuse over distances of several nanometers in the

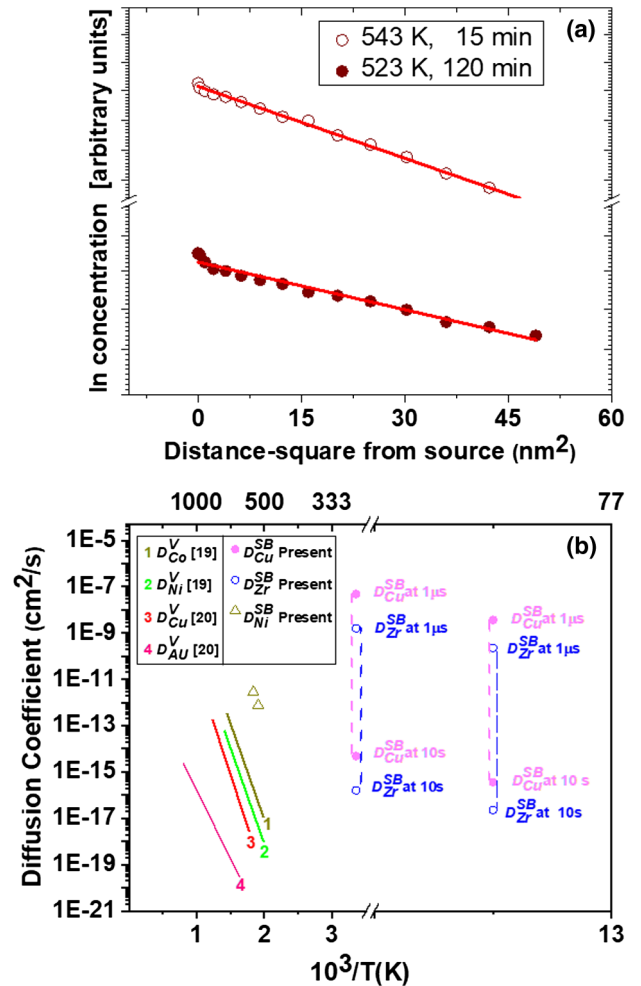


FIG. 3. (a) Typical plots of  $\log C$  versus  $z^2$  for the diffusion of Ni along the shear band of Cu-Zr metallic glass. The solid lines represent fits according to Eq. (1). (b) Temperature dependence of different diffusion coefficients in amorphous binary metallic glasses. The diffusion coefficients of Cu and Zr in the shear bands at RT and 80 K are indicated in the graphs with an estimated window of diffusion time. These values are compared to the diffusion volume coefficients ( $D^V$ ) in the homogeneous metallic glasses available for the  $\text{Ni}_{50}\text{Zr}_{50}$  system [17,18].

center of the modified region within the shear band, and do not follow the asymmetric profile of the Cu atoms, although the size and diffusion behavior of Ni and Cu have been reported to be similar. This indicates that the self-diffusion of Cu and Zr during the shear band motion follows a different behavior than the Ni tracer diffusion. From this observation, it is concluded that the diffusion of Ni atoms in the shear band can be described in analogy to grain boundary diffusion in crystalline or nanocrystalline materials as described by Harrison's C-type kinetics regime [19]. The mathematical description of the concentration for the source-grain boundary-bulk model initiated by Fisher [20] can be applied also for the source-shear band case as follows:

$$C(z) = C_0 \exp\left(\frac{z^2}{4D^{\text{SB}}_t}\right), \quad (1)$$

where  $C_0$ ,  $C(z)$ , and  $t$  define the initial concentration, the concentration at a depth  $z$ , and the diffusion time, respectively. The coordinate  $z$  is taken along the shear band to determine the short-circuit diffusion coefficient  $D^{\text{SB}}$ .

From the elemental maps across the shear band, the Ni concentration at various depth is determined and plotted in Fig. 3(a) for the two temperatures of the measurement. The obtained profiles agree well with the analytical solutions proposed in Eq. (1), and the plotted slopes after different annealing times and temperatures are compatible with the expected time dependence. The linearity of the plot  $\log C$  versus  $z^2$  confirms the  $C$  regime. As a result, the shear band diffusion coefficients of Ni tracer in Cu-Zr metallic glass can be reliably determined ( $D^{\text{SB-Ni}}_{T=523\text{ K}} = (8.71 \pm 1.6) \times 10^{-13}$  cm<sup>2</sup>/s,  $D^{\text{SB-Ni}}_{T=543\text{ K}} = (3.07 \pm 2.1) \times 10^{-12}$  cm<sup>2</sup>/s).

The characterization of elemental distribution outside and within the shear bands of Cu<sub>50</sub>Zr<sub>50</sub> using APT leads to the following main observations:

(A) The nondeformed regions showed very little compositional fluctuation while the shear band region showed massive changes in composition. In order to obtain some rough estimate of the increased diffusion coefficients during shear band motion, two values of the time are used as the lower and upper limit. As a value for the shortest time it is assumed that the diffusion exclusively occurs during the motion of the shear band, i.e., 1  $\mu$ s. For the longest time, 10 s is assumed. This leads to a range of diffusion coefficients given in Fig. 3(b) between 10<sup>-8</sup> and 10<sup>-15</sup> cm<sup>2</sup>/s. Although this is a rather wide band, it still demonstrates that the diffusion within the shear bands is drastically enhanced compared to the diffusion measured in a homogeneous glass. Even an extension of the diffusion time to the longest value possible, the time between the deformation and the APT measurement, which is typically 24 h, does not bring the diffusion values in the shear bands to the values of the thermal diffusion in the homogeneous glass structure. A drastic temperature increase during the shear band motion is one of the most common plausible explanations [14]. However, some reports [21,22] have claimed that the temperature rise is only in the order of just a few kelvin during indentation and compression, and the reason for such enhanced atomic mobility is because of the flow dilatation in the shear band resulting in higher diffusion coefficients without any drastic increase in temperature. In our results, a clear phase separation perpendicular to the direction of shear band motion is observed, which indicates that shear alone cannot explain the observed elemental redistribution. Intuitively, shear can produce gradients along the direction of motion, while temperature can generate concentration gradients along the perpendicular direction of shear band motion. Therefore, we can speculate that the reason for such an enhanced

diffusion coefficient is most likely a combination of both temperature and stress.

(B) The changes of the elemental distribution across the shear band depend on the deformation temperature (80 K and RT), but the occurrence of concentration variations even at a sample temperature of 80 K indicates that the temperature during the motion of the shear band is higher. By means of correlative APT and TEM in plastically deformed Al<sub>85.6</sub>Y<sub>7.5</sub>Fe<sub>5.8</sub> metallic-glass ribbons, Balachandran *et al.* [23] showed the existence of two distinct regions dominated by Al enrichment and Al depletion, which is similar to the data reported in the present work. However, our study clearly reveals that such redistribution could be reduced at low temperatures. This could play a significant role in the ductile-brittle transition in metallic glasses observed at low temperatures [24].

(C) The changes of the concentration profiles of Cu and Zr in the shear band regions during annealing at a temperature up to 543 K, i.e., at a homologous temperature of  $\sim 0.8$  ( $T_g = 683$  K), are negligible. This indicates that the structural changes within the shear band are stable under these annealing conditions. In general, one can assume that the diffusivity at 523 and 543 K should be sufficiently fast to lead to the homogeneous distribution, if the thermodynamic driving force would mandate it. According to the Cu-Zr phase diagram, the equilibrium phases for a Cu<sub>50</sub>Zr<sub>50</sub> glass after crystallization are Cu<sub>10</sub>Zr<sub>7</sub> and CuZr<sub>2</sub>. The concentration fluctuations in the shear band are in a similar range, which indicates that the shear band is undergoing phase separation like processes to attain a lower equilibrium state. The present self-diffusion results are also consistent with atomistic simulations computed in deformed Cu-Zr metallic glass, which observed enhancement of the Cu-Cu and Zr-Zr bonds inside the shear bands with respect to that of the undeformed bulk [25].

(D) The preferred diffusion of a Ni tracer along the shear band clearly shows that the necessary atomic mobility exists within the band and is substantially fast with very little diffusion into the undeformed matrix. The Ni diffusion is occurring within the center of the asymmetric distributions of Cu and Zr, and seems not to follow the Cu profile. The distribution of the Ni tracer across the shear band is rather narrow, confined to only 2 nm, not wider than the Cu and Zr profiles. From Fig. 3(b) it is clearly seen that the diffusion coefficients of Ni along the shear band at the two temperatures (523 and 543 K) are at least 8 orders of magnitude faster than comparable values of Ni and Cu diffusion in a homogeneous Ni<sub>50</sub>Zr<sub>50</sub> glass [17,18]. Unfortunately, no direct comparison of diffusion data in the same material system (Cu<sub>50</sub>Zr<sub>50</sub>) is possible due to the lack of reported values. However, the chemical nature and the atomic size of Cu and Ni are rather similar, and thus it is assumed that the diffusion coefficients are also comparable, at least considering the data on the ‘‘order-of-magnitude’’ level. Similar magnitudes of diffusion were reported by

Bokeloh *et al.* [9] indicating that the fast diffusion paths are preferentially present in the shear bands. The authors also speculated that the preferred high-mobility pathways could be along the center of the band or at the interface between the shear band and the matrix. The present study clearly shows that the shortcut diffusion seems to happen through the center of the band rather than the interfaces between the bands and undeformed matrix. In this context, one can draw the analogy of diffusivity in shear bands to that of the grain boundary diffusion in nanocrystalline materials, which shows comparable values of diffusion coefficients [13,26]. To date, the physical mechanisms responsible for these compositional and density changes as well as short-circuit diffusion path taking place within the shear bands are yet to be fully understood.

In conclusion, the shear bands represent an amorphous structure, which seems to be different in composition and other aspects (stress fields, free volume) from the amorphous structure of surrounding matrix. We observed abrupt enhancement of Cu and Zr diffusivities toward opposite sides along the thickness of the shear band. Diffusion during the formation of the shear bands is drastically increased, which most likely is a consequence of the temperature rise and the plastic deformation occurring during shear band motion. The persistence of inhomogeneous atomic structure within the shear band even at a homologous temperature of 0.8 is demonstrated by the stability of Cu and Zr profiles. The increased diffusion coefficient of a Ni tracer, which is at least 8 orders of magnitude faster in the narrow shear band region compared to the homogeneous metallic glass, clearly indicates the presence of enhanced free volume inside the band. Our results also unequivocally demonstrate that the diffusion happens through the center of the shear band rather than the interface between the shear band and the matrix.

The authors are grateful to the Karlsruhe Nano Micro Facility (KNMF) for support and access to APT and FIB facilities. M. R. C. acknowledges the financial support received from the Karlsruhe Institute of Technology (KIT). S. H. N. and H. H. would like to thank the DFG/SPP 1594 program for funding the projects HA1344/30-1 and HA1344/46-1. The authors would like to thank Professor Virgil Provenzano for constructive criticism of the manuscript.

\*Corresponding author.

mohammed.chellali@kit.edu

- [1] V. Schmidt, H. Rösner, M. Peterlechner, G. Wilde, and P. M. Voyles, Quantitative Measurement of Density in a Shear Band of Metallic Glass Monitored along Its Propagation Direction, *Phys. Rev. Lett.* **115**, 035501 (2015).
- [2] E. R. Homer, Examining the initial stages of shear localization in amorphous metals, *Acta Mater.* **63**, 44 (2014).
- [3] D. Şopu, A. Stukowski, M. Stoica, and S. Scudino, Atomic-Level Processes of Shear Band Nucleation in Metallic Glasses, *Phys. Rev. Lett.* **119**, 195503 (2017).
- [4] A. Y. Vinogradov and V. Khonik, Kinetics of shear banding in a bulk metallic glass monitored by acoustic emission measurements, *Philos. Mag.* **84**, 2147 (2004).
- [5] D. Klaumünzer, A. Lazarev, R. Maaß, F. Dalla Torre, A. Vinogradov, and J. F. Löffler, Probing Shear-Band Initiation in Metallic Glasses, *Phys. Rev. Lett.* **107**, 185502 (2011).
- [6] S. Hilke, H. Rösner, D. Geissler, A. Gebert, M. Peterlechner, and G. Wilde, The influence of deformation on the medium-range order of a Zr-based bulk metallic glass characterized by variable resolution fluctuation electron microscopy, *Acta Mater.* **171**, 275 (2019).
- [7] A. Bartsch, K. Rätzke, A. Meyer, and F. Faupel, Dynamic Arrest in Multicomponent Glass-Forming Alloys, *Phys. Rev. Lett.* **104**, 195901 (2010).
- [8] S. P. Singh, M. R. Chellali, L. Velasco, Y. Ivanisenko, E. Boltynjuk, H. Gleiter, and H. Hahn, Deformation-induced atomic rearrangements and crystallization in the shear bands of a Tb<sub>75</sub>Fe<sub>25</sub> nanoglass, *J. Alloys Compd.* **821**, 153486 (2020).
- [9] J. Bokeloh, S. V. Divinski, G. Reglitz, and G. Wilde, Tracer Measurements of Atomic Diffusion inside Shear Bands of a Bulk Metallic Glass, *Phys. Rev. Lett.* **107**, 235503 (2011).
- [10] P. Kersch, U. Rössler, B. Idzikowski, A. Handstein, K. Nenkov, N. Mattern, K.-H. Müller, and L. Schultz, Phase formation in the 1–6–6 pseudobinary system Dy(Mn<sub>6</sub>Ge<sub>6</sub>)<sub>1-x</sub>(Fe<sub>6</sub>Al<sub>6</sub>)<sub>x</sub>, *Mater. Sci. Eng. A* **375**, 516 (2004).
- [11] See Supplemental Material at <http://link.aps.org/supplemental/10.1103/PhysRevLett.125.205501> for the APT sample preparation and the 3D reconstruction of the undeformed and deformed Cu<sub>50</sub>Zr<sub>50</sub> ribbon. The concentration profiles taken in the bulk and the shear band are also shown.
- [12] M. Chellali, L. Zheng, R. Schlesiger, B. Bakhti, A. Hamou, J. Janovec, and G. Schmitz, Grain boundary segregation in binary nickel-bismuth alloy, *Acta Mater.* **103**, 754 (2016).
- [13] M. R. Chellali, Z. Balogh, H. Bouchikhaoui, R. Schlesiger, P. Stender, L. Zheng, and G. Schmitz, Triple junction transport and the impact of grain boundary width in nanocrystalline Cu, *Nano Lett.* **12**, 3448 (2012).
- [14] J. Lewandowski and A. Greer, Temperature rise at shear bands in metallic glasses, *Nat. Mater.* **5**, 15 (2006).
- [15] K. Maier, Self-diffusion in copper at “low” temperatures, *Phys. Status Solidi (a)* **44**, 567 (1977).
- [16] H. Hahn and R. S. Averback, Dependence of tracer diffusion on atomic size in amorphous Ni-Zr, *Phys. Rev. B* **37**, 6533 (1988).
- [17] K. Hoshino, R. S. Averback, H. Hahn, and S. J. Rothman, Tracer diffusion of <sup>60</sup>Co and <sup>63</sup>Ni in amorphous NiZr alloy, *J. Mater. Res.* **3**, 55 (1988).
- [18] H. Hahn, R. S. Averback, and S. Rothman, Diffusivities of Ni, Zr, Au, and Cu in amorphous Ni-Zr alloys, *Phys. Rev. B* **33**, 8825 (1986).
- [19] L. Harrison, Influence of dislocations on diffusion kinetics in solids with particular reference to the alkali halides, *Trans. Faraday Soc.* **57**, 1191 (1961).

- [20] J. C. Fisher, Calculation of diffusion penetration curves for surface and grain boundary diffusion, *J. Appl. Phys.* **22**, 74 (1951).
- [21] S. K. Slaughter, F. Kertis, E. Deda, X. Gu, W. J. Wright, and T. C. Hufnagel, Shear bands in metallic glasses are not necessarily hot, *APL Mater.* **2**, 096110 (2014).
- [22] J.-J. Kim, Y. Choi, S. Suresh, and A. Argon, Nanocrystallization during nanoindentation of a bulk amorphous metal alloy at room temperature, *Science* **295**, 654 (2002).
- [23] S. Balachandran, J. Orava, M. Köhler, A. J. Breen, I. Kaban, D. Raabe, and M. Herbig, Elemental re-distribution inside shear bands revealed by correlative atom-probe tomography and electron microscopy in a deformed metallic glass, *Scr. Mater.* **168**, 14 (2019).
- [24] F. H. Dalla Torre, A. Dubach, J. Schällibaum, and J. F. Löffler, Shear striations and deformation kinetics in highly deformed Zr-based bulk metallic glasses, *Acta Mater.* **56**, 4635 (2008).
- [25] Y. Ritter and K. Albe, Chemical and topological order in shear bands of  $\text{Cu}_{64}\text{Zr}_{36}$  and  $\text{Cu}_{36}\text{Zr}_{64}$  glasses, *J. Appl. Phys.* **111**, 103527 (2012).
- [26] H. Joubert, J. Terblans, and H. Swart, Determining the diffusion coefficient of Ni in Cu from a Ni/Cu thin film using linear heating, scanning Auger microscopy and a numerical solution of Fick's second law, *Surf. Interface Anal.* **42**, 1213 (2010).